



## Synthesis and characterization of new amorphous and crystalline phases in $\text{Bi}_2\text{O}_3\text{-Ta}_2\text{O}_5\text{-TeO}_2$ system

Imane Yakine\*, Abdeslam Chagraoui, Abdenajib Moussaoui, Abdelmjid Tairi

Laboratoire de Chimie Analytique et Physico-Chimie des Matériaux, Faculté des Sciences Ben M'sik, Université Hassan II-Mohammedia Casablanca (Morocco).

Received 3 March 2012, Revised March 2012, Accepted March 2012

\* Corresponding author: [imane.yakine85@gmail.com](mailto:imane.yakine85@gmail.com)

### Abstract

A glass-forming domain is found and studied within  $\text{Bi}_2\text{O}_3\text{-Ta}_2\text{O}_5\text{-TeO}_2$  system. The glasses obtained in the system  $\text{Ta}_2\text{O}_5\text{-TeO}_2$  was investigated by DSC, Raman and Infrared spectroscopy. The influence of a gradual addition of the modifier oxides  $\text{Ta}_2\text{O}_5$  on the coordination geometry of tellurium atoms has been elucidated based Infrared and Raman studies and showed the transition of  $\text{TeO}_4$ ,  $\text{TeO}_{3+1}$  and  $\text{TeO}_3$  units with increasing  $\text{Ta}_2\text{O}_5$  content. The density of glasses has been measured. The investigation in the  $\text{TeO}_2\text{-Ta}_2\text{O}_5$  system using XRD reveals new phases.

**Keywords:** X Ray Diffraction -DSC - IR- Glass transition - Tellurite glasses

### 1. Introduction

The enhanced nonlinear optical materials have attracted much interest with novel applications in optoelectronics, optical switchers and limiters, as well as in optical computers, optical memory, and nonlinear spectroscopy. Tellurite glasses, due to their wide infrared window, excellent chemical durability and stability, ultra-fast nonlinear optical response and excellent third-order optical nonlinearity, have noticeable advantages in comparison with other conventional glasses, which make the tellurite glasses especially attractive in a variety of practical applications. Recently, the interest on tellurite glasses is focused on their high refractive index. Tellurite glasses in the systems such as  $\text{TeO}_2\text{-Nb}_2\text{O}_5$ ,  $\text{TeO}_2\text{-Nb}_2\text{O}_5\text{-ZnO}$ ,  $\text{TeO}_2\text{-Bi}_2\text{O}_3\text{-ZnO}$ ,  $\text{TeO}_2\text{-TiO}_2\text{-BaO}$ ,  $\text{TeO}_2\text{-TiO}_2\text{-Bi}_2\text{O}_3$  and  $\text{TeO}_2\text{-TiO}_2\text{-Nb}_2\text{O}_5$  have been demonstrated to have excellent nonlinear optical performances [1–6]. Therefore, abundant researches are focused on producing new tellurite glasses of improved optical properties.

The present paper reports a preliminary investigation of new tellurite glasses and crystalline phases in  $\text{Bi}_2\text{O}_3\text{-Ta}_2\text{O}_5\text{-TeO}_2$  system. Elaboration process, thermal properties infrared (IR) and Raman studies in comparison to analogous crystalline phases will be described successively.

### 2. Experimental

The amorphous and crystalline samples were prepared using high purity commercial materials  $\text{Bi}_2\text{O}_3$ ,  $\text{TeO}_2$ ,  $\text{Ta}_2\text{O}_5$  of analytical grade (Aldrich 99.9%). The batches of suitable proportions of starting products were mixed in an agate mortar and then heated in air at  $800^\circ\text{C}$  (20 min) for vitreous phases and at  $600^\circ\text{C}\text{-}800^\circ\text{C}$  (48h) for crystalline phases. All of them are quenched to room temperature and identified by X-ray diffraction (XRD) using a Bruker D8 Advance diffractometer (Cu-K-alpha radiation).  $T_g$  (glass temperature) and  $T_c$  (crystallization temperature) were determined using Differential Scanning Calorimetry (DSC) Netsch 2000 PC

type from powder samples glasses for about 8mg in aluminum pans. A heating rate of 10°C/min was used in the 30-650°C range. Infrared absorption measurements between 2000-400 cm<sup>-1</sup> were made for powder specimens dispersed in a pressed KBr disk. The Raman spectra were recorded in the 80-1000 cm<sup>-1</sup> range using a Jobin-Yvon spectrometer (64000 model) equipped with an Ar+ laser (514.5 nm exciting line) and a CCD detector in a backscattering geometry. The sample focalization was controlled through a microscope (×100). The diameter of the laser spot focused on the sample was about 1 mm. The spectra were recorded in two scans (during 100 s) at low power (<100 mW) of the excitation line, in order to avoid damage of the glasses. The spectral resolution was about 2.5 cm<sup>-1</sup> at the exciting line. The densities of samples were measured according to the Archimedes's principle using diethylorthophtalat as solvent.

### 3. Results and discussion

A wide range glass system based on the Bi<sub>2</sub>O<sub>3</sub>-Ta<sub>2</sub>O<sub>5</sub>-TeO<sub>2</sub> system was prepared at 800°C after a series of composition. the vitreous was determined by X-ray diffraction . This temperature have been chosen to have a homogenous reagent in one hand and to avoid volatization of TeO<sub>2</sub> at high temperature (T<sub>TeO2Melting</sub>=732°C) on the other hand (Figure 1). The color of the glass changes slightly from dark yellow to yellow with increasing Ta<sub>2</sub>O<sub>5</sub> and Bi<sub>2</sub>O<sub>3</sub> concentration.

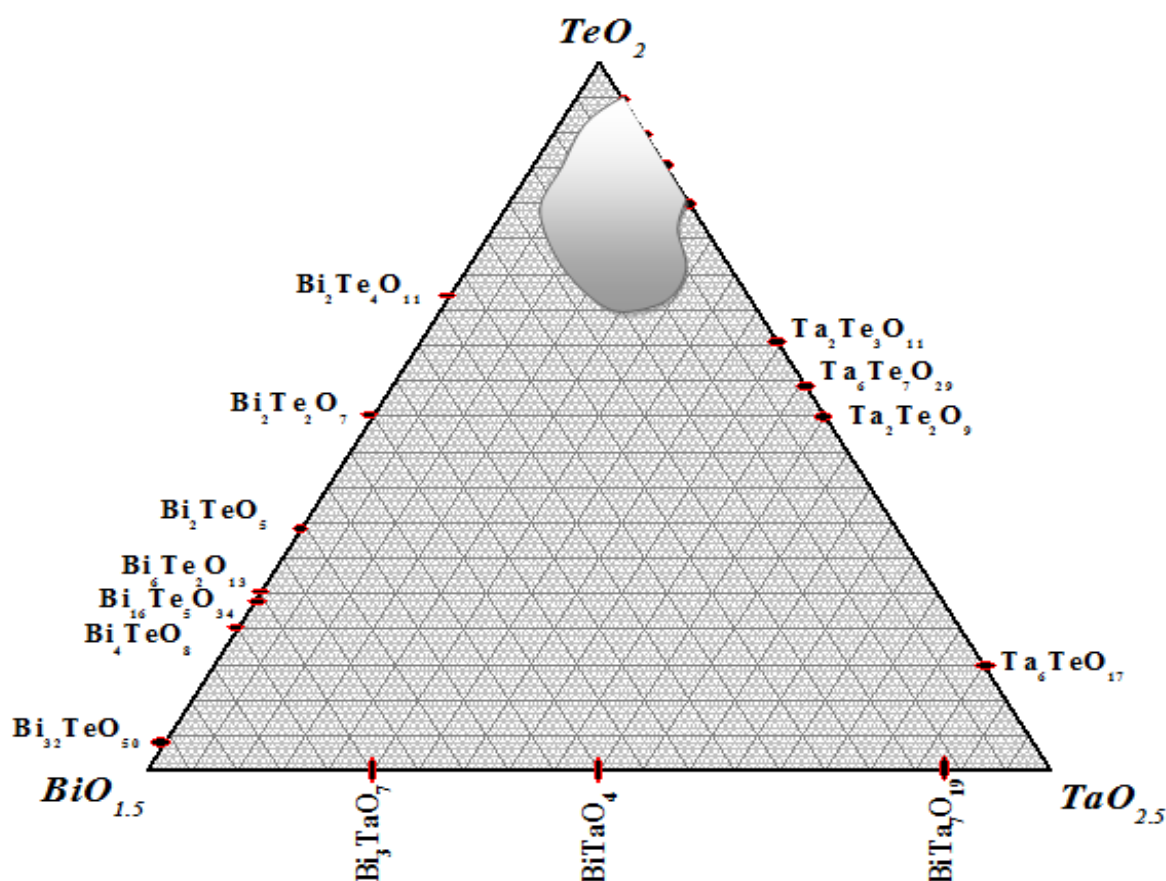


**Figure 1:** Vitreous domain diagram for the Bi<sub>2</sub>O<sub>3</sub>-TeO<sub>2</sub>-Ta<sub>2</sub>O<sub>5</sub> system

#### 3.1. Differential scanning calorimetry(DSC)

Series of glasses composition are listed in (Table 1). An addition of TaO<sub>2.5</sub> (up to 0.5 mol%) would result in the increase of glass stability (as indicated by T<sub>c</sub>-T<sub>g</sub>). This is presumably due to the participation of Ta<sup>5+</sup> in the glass network. The values of T<sub>g</sub>, T<sub>c1</sub>, T<sub>c2</sub> and T<sub>c3</sub> are presented (Figure 2) and (Table 1).

**Table 1:** Characteristics ( $T_g$ ,  $T_c$ ) and difference ( $T_{c1} - T_g$ ) of some glasses in the  $Ta_2O_5$ - $TeO_2$ - $Bi_2O_3$  system.

% $TeO_2$	% $TaO_{2.5}$	$T_g$ (°C)	$T_{c1}$ (°C)	$T_{c2}$ (°C)	$T_{c3}$ (°C)	$T_{c1}-T_g$ (°C)
95	5	378	490	522	595	112
90	10	380	412	518	572	38
85	15	382	461	516	576	79

The curves (DSC) exhibit an endothermic effect due to glass transition ( $T_g$ ), and shows that three exothermic phenomenon occurred at ( $T_{c1}$ ), ( $T_{c2}$ ) and ( $T_{c3}$ ), due to the formation of different crystalline phases. The appearance of single peak (all glasses) due to the glass transition temperature  $T_g$  indicates the homogeneity of the glasses prepared. With increasing of  $Ta_2O_5$  content in the glass matrix, the  $T_g$  increases and the difference ( $T_c - T_g$ ) (about 79-112°C) implies a thermal stability of glasses (Figure 2).

In a study of alkali tellurite glasses, Pye et al [7] showed that the temperature of the glass transition decreases with increasing amount of Li, Na or K compound. The dependence of  $Ta_2O_5$  content shows a different tendency especially of glass transition compared with the alkali tellurite glasses. The alkali atoms easily move in the glass structure. The slight change of the temperature of crystallization of a vitreous composition to another is due to the kinetic phenomenon. Based on XRD and DSC analysis for glassy samples 5-20 mol %  $TaO_{2.5}$  (Figure 3a). The first peak of crystallization corresponds to the  $\gamma TeO_2$ ,  $\alpha TeO_2$  and  $Ta_2Te_3O_{11}$  at 500°C. This phenomenon which we observed, i.e. the crystallization of  $\gamma TeO_2$  variety is also obtained in the many systems as  $TeO_2$ - $WO_3$  [10],  $Nb_2O_5$ - $TeO_2$  [8,11],  $TeO_2$ - $ZnO$  [12],  $TeO_2$ - $SrO$  [13] and  $Sb_2O_3$ - $TeO_2$  [14]. In second crystallization at 550°C belongs to reinforcing  $Ta_2Te_3O_{11}$  and  $\alpha TeO_2$  phases. The last peak (650°C) with weak intensity is attributed to totally transformation  $\gamma TeO_2$  metastable polymorph into the stable  $\alpha TeO_2$  and  $Ta_2Te_3O_{11}$ .

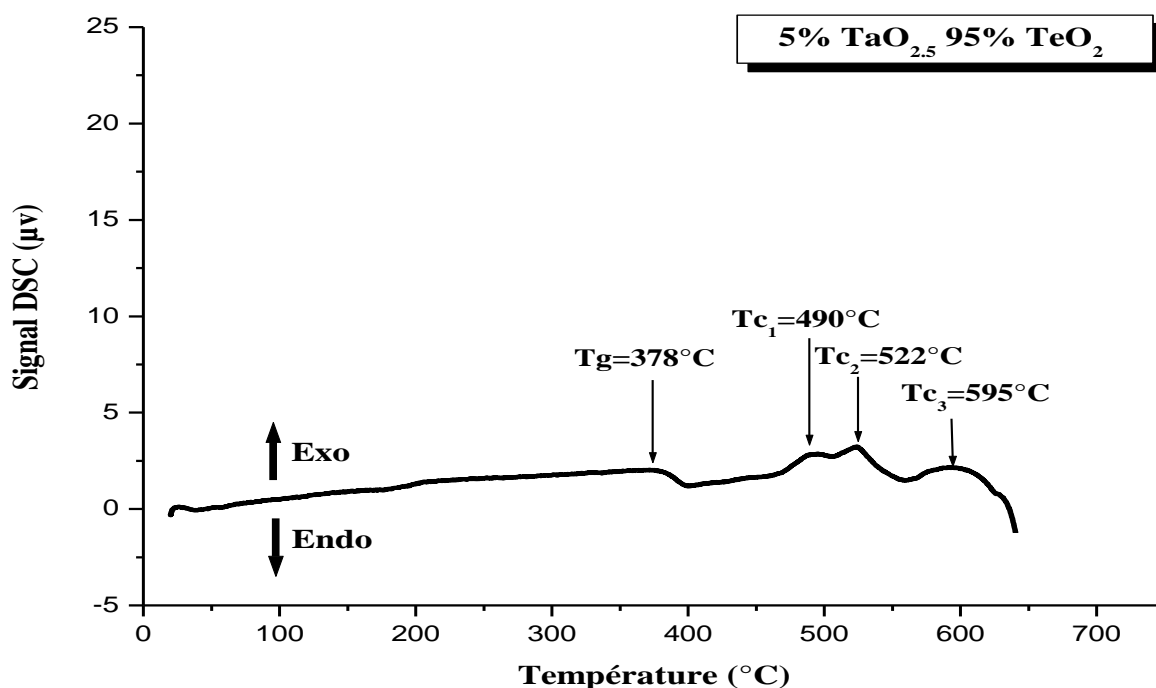


**Figure 2 :** DSC curves of glassy samples obtained in  $xTaO_{2.5}$ ,  $(1-x)TeO_2$  pseudo- binary ( $0.05 \leq x \leq 0.15$ )

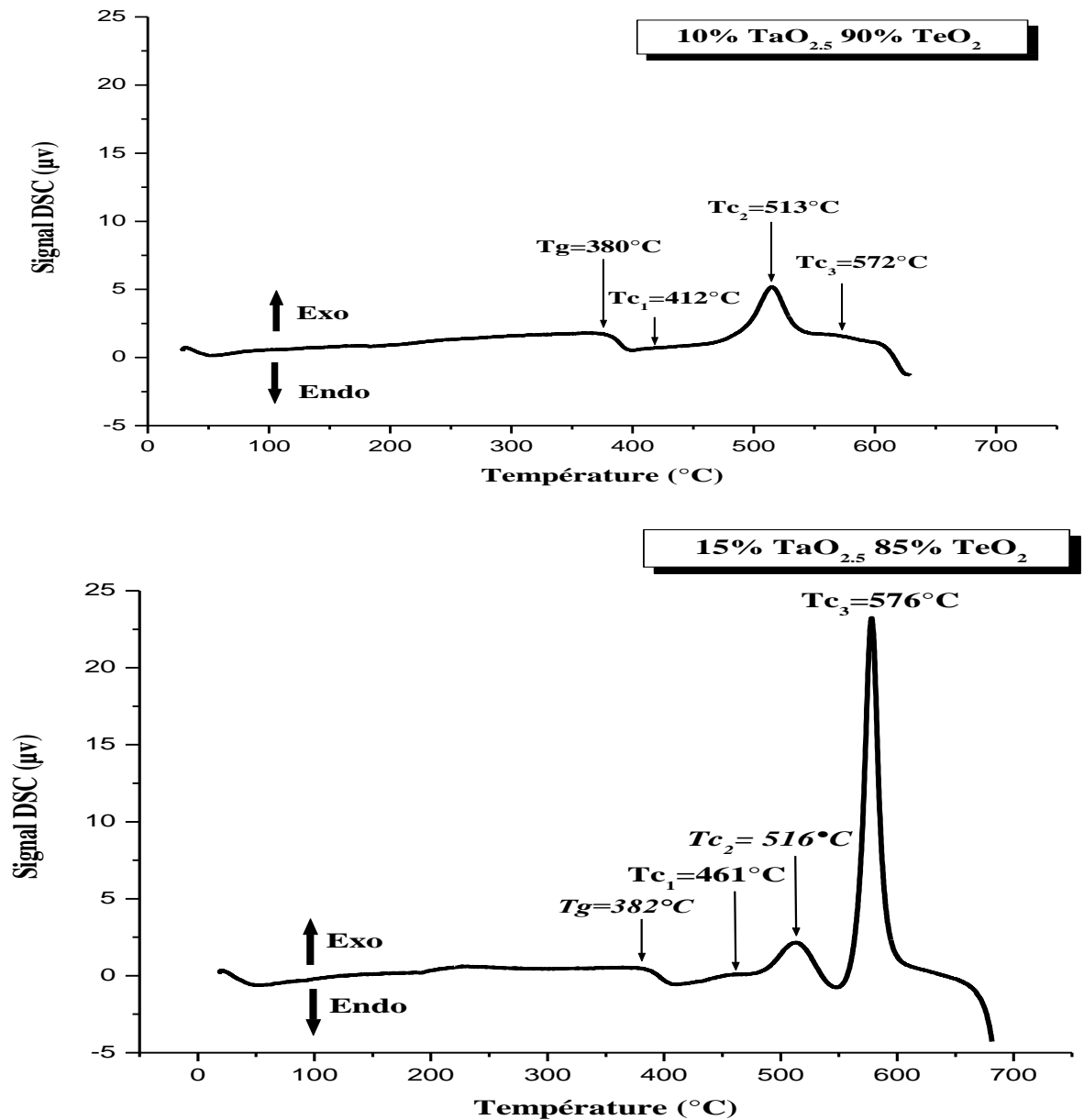


**Figure 2bis :** DSC curves of glassy samples obtained in  $x\text{TaO}_{2.5}$ ,  $(1-x)\text{TeO}_2$  pseudo- binary ( $0.05 \leq x \leq 0.15$ )

It is important to mention that the thermal analysis curves discussed in paragraph 3-1 of glasses of the pseudo – binary  $\text{TeO}_2 - \text{TaO}_{2.5}$  which have a composition of 15 % mol of  $\text{TaO}_{2.5}$  exhibit three crystallizations, there X ray diffraction data are plotted in (Figure 3b). The first crystallization occurred within the range of  $400^\circ\text{C}$  and  $490^\circ\text{C}$ , the X ray diffraction spectra of the crystallized phases gained after a thermal annealing of the composition (85 %  $\text{TeO}_2$ , 15%  $\text{TaO}_{2.5}$ ) at temperature  $500^\circ\text{C}$  during 24h, shows the existence of a tri-phases mixture:  $\text{TeO}_2(\alpha)$ ,  $\text{TeO}_2(\beta)$  and a new phase called Y.

The second crystallization occurred within the range of  $450^\circ\text{C}$  and  $540^\circ\text{C}$ , a new phase Y showed up after a thermal annealing of the same composition used in the first process of crystallization at a temperature of  $500^\circ\text{C}$  during 24h and disparities of  $\text{TeO}_2(\alpha)$  and  $\text{TeO}_2(\gamma)$  phases. Finally, the third crystallization which happened within the range of  $550^\circ\text{C}$  and  $640^\circ\text{C}$  and which was thermally annealed at  $650^\circ\text{C}$ , exhibits the same behavior as that of second one.

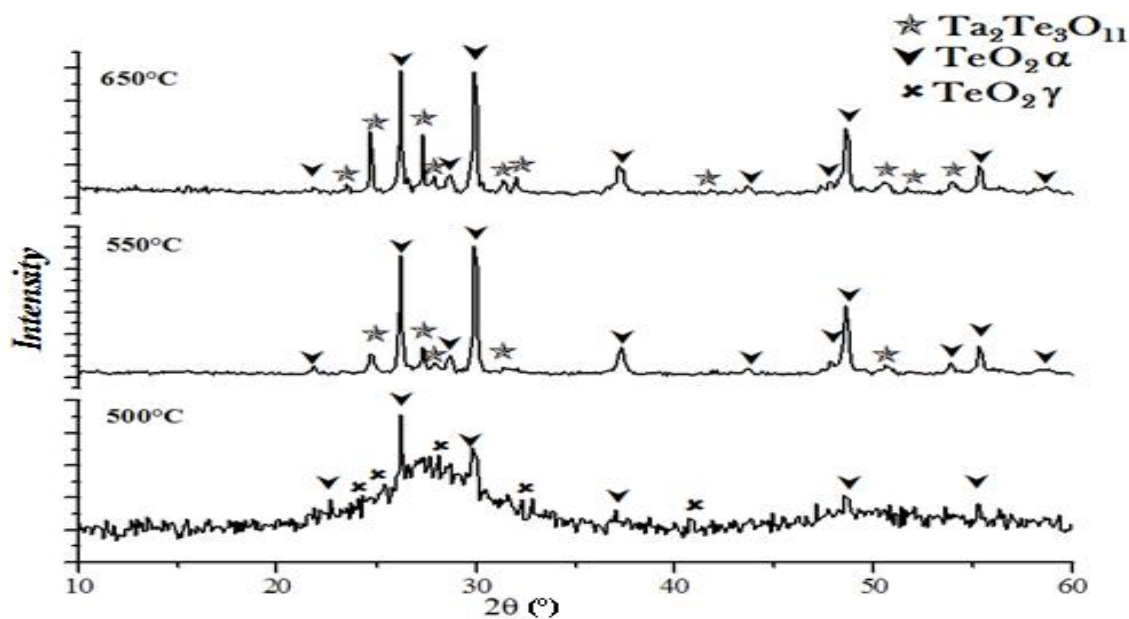


**Figure 3a:** XRD patterns heat-treated at 500°C, 550°C and 650°C of (90%TeO<sub>2</sub>,10% TaO<sub>2.5</sub> mol) in pseudo-binary TeO<sub>2</sub>- TaO<sub>2.5</sub>.

The automatic peaks indexation of this new phase Y using program ito [15], provided the following results:  $M(12) = 81$  on the basis of monoclinic lattice with  $a=7.05 \text{ \AA}$ ,  $b=8.946 \text{ \AA}$ ,  $c=6.434 \text{ \AA}$ ,  $\beta= 100.54^\circ$  and  $V_{\text{lattice}} = 398.94 \text{ \AA}^3$ . The reflection conditions are in agreement with space groups  $C_c$  and  $C_{2/c}$ . The indexed powder diffraction pattern is shown in (Table 2). The structural characterization of this phase will be published future article.

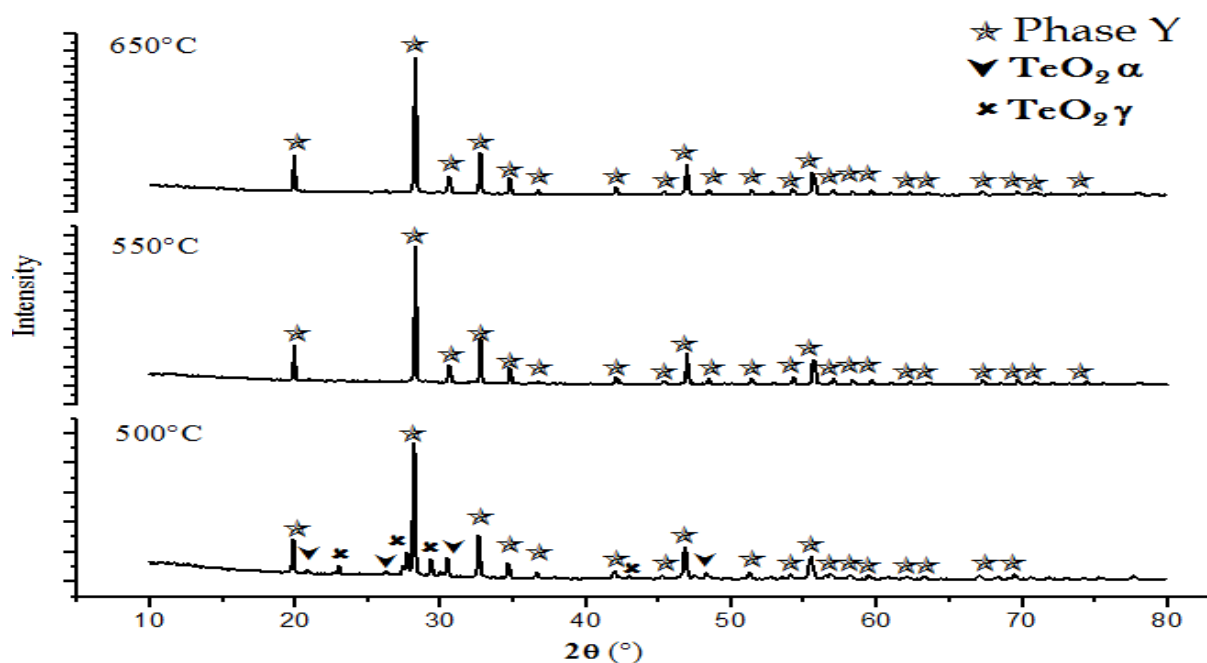


**Figure 3b:** XRD patterns heat-treated at 500°C, 550°C and 650°C of (85%TeO<sub>2</sub>,15% TaO<sub>2.5</sub> mol) in pseudo-binary TeO<sub>2</sub>-TaO<sub>2.5</sub>.

**Table 2:** Indexing of XRD reflections of new phase Y.

<i>h k l</i>	<i>d<sub>obs</sub></i> (Å)	<i>d<sub>cal</sub></i> (Å)	<i>I/I<sub>o</sub></i>
1 1 -1	4.454	4.452	28
0 0 2	3.153	3.152	100
1 1 -2	2.919	2.919	15
2 2 0	2.732	2.731	33
1 1 2	2.575	2.576	12
1 3 1	2.443	2.444	4
2 0 2	2.143	2.144	6
3 1 1	1.996	1.997	3
2 2 2	1.933	1.933	20
1 1 3	1.875	1.876	5
2 2 4	1.714	1.713	5
3 1 -3	1.688	1.688	5
1 5 1	1.649	1.650	18
4 2 0	1.613	1.613	5
0 0 4	1.579	1.579	4
2 0 -4	1.547	1.548	4
0 2 4	1.489	1.489	2
1 1 4	1.462	1.462	4
5 1 -1	1.390	1.390	4
2 0 4	1.347	1.347	4
1 3 4	1.327	1.327	3
5 3 -1	1.273	1.273	3

### 3.2. Density and molar volume

#### 3.2.1. Experiment procedure

The density of the specimens was measured using Archimedes principle using orthophthalate as the immersion liquid ( $d_{\text{orthophthalate}} = 1.11573$  at 23.5°C). A glass disc was weighted in air ( $W_{\text{air}}$ ) and immersed in orthophthalate and reweighted ( $W_{\text{orthophthalate}}$ ). The relative density is given by the following relation [16]:

$$d = d_{\text{orthophthalate}} \frac{W_{\text{air}}}{W_{\text{orthophthalate}}}$$

The data from the performed measurements are shown in (Table 3). Moreover, the variation of the density and the molar volume of some composition the pseudo – binary  $\text{TeO}_2\text{-TaO}_{2.5}$  vitreous phases versus the added amount of  $\text{TaO}_{2.5}$  is illustrated in (Figure 4).

According to the plotted data in (Figure 4), it is obvious that the density of the vitreous phases of the pseudo – binary  $\text{TeO}_2\text{-TaO}_{2.5}$  increases as the rate of  $\text{TaO}_{2.5}$  increases. However, the molar volume decrease with that same rate of  $\text{TaO}_{2.5}$  according to increasing  $T_g$ . The explanation can provided of this rise of the density lies in the difference between the molar masses of the elements ( $M_{\text{TaO}_{2.5}} > M_{\text{TeO}_2}$ ). Besides, we suppose that the exhibited decrease of molar volume ( $M$ ) is due to the contraction of the vitreous network, caused by the added  $\text{TaO}_{2.5}$ .

**Table 3:** Density, and molar volume of some composition the pseudo – binary TeO<sub>2</sub>-TaO<sub>2.5</sub>

%mol TeO <sub>2</sub>	% mol TaO <sub>2.5</sub>	Density ( $\pm 0,02$ )	molar volume (M)( $\text{\AA}^3$ )
95	5	6.10	26.67
90	10	6.25	26.49
85	15	6.41	26.33
80	20	6.57	26.15

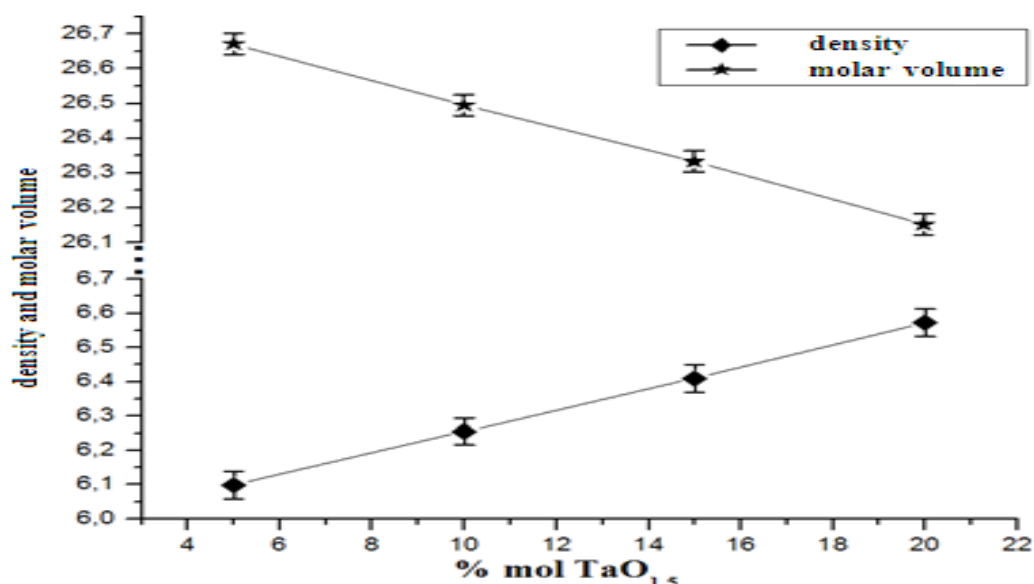


**Figure 4:** Variation of the density and that of the molar volume of some of the pseudo – binary TeO<sub>2</sub>-TaO<sub>2.5</sub>

### 3.3 Spectroscopy studies

#### 3.3.1 IR study

The bands in the IR spectrum of crystalline TeO<sub>2</sub> are assigned according to C<sub>2v</sub> point group symmetry in the following manner:

$\nu(\text{Te-O}_{\text{eq}}^{\text{s}}) = 780 \text{ cm}^{-1}$ ,  $\nu(\text{Te-O}_{\text{eq}}^{\text{as}}) = 714 \text{ cm}^{-1}$ ,  $\nu(\text{Te-O}_{\text{ax}}^{\text{as}}) = 675 \text{ cm}^{-1}$  et  $\nu(\text{Te-O}_{\text{ax}}^{\text{s}}) = 635 \text{ cm}^{-1}$ .

In the pure TeO<sub>2</sub> glass the  $\nu^{\text{s}}$  band at  $635 \text{ cm}^{-1}$  increases markedly instated of  $\nu^{\text{as}}$  TeOax =  $675 \text{ cm}^{-1}$  and becomes a determining one. The rise of  $\nu_{\text{ax}}^{\text{s}}$  intensity is the result of decrease in the symmetry of the polyhedra in the glass network [17-19].

IR spectra of tellurite built up by TeO<sub>3</sub> polyhedra with equal lengths of the Te-O show four normal vibrations. Two of them  $\nu(\text{A}_1)$  and  $\nu(\text{E})$  correspond to the symmetric ( $\nu^{\text{s}}$ ) and degenerate ( $\nu^{\text{d}}$ ). The polyhedra are assigned to the point group C<sub>3v</sub> [20,21].

The infrared transmission spectrum of glasses in TaO<sub>2.5</sub>-TeO<sub>2</sub> system (Figure 5) exhibits vibrational bands in the range  $600\text{--}800 \text{ cm}^{-1}$ . This region may also consist of bands due to anti-symmetrical and symmetrical vibrations of TeO<sub>2</sub>. For (5% TaO<sub>2.5</sub> content) an intense band is observed nearly at  $671 \text{ cm}^{-1}$  when compared with crystal (TeO<sub>2</sub>). It characterizes the presence of non-symmetrical TeO<sub>4</sub> groups which give an indication



that tellurium does not change its coordination number four in this range of compositions. This band  $671\text{cm}^{-1}$  is attributed to the asymmetric vibrations in  $\text{O}_{\text{ax}}\text{-Te-O}_{\text{ax}}$  groups into  $\text{TeO}_4$  polyhedra. It is progressively broadening and moving towards the higher energy with  $\text{TaO}_{2.5}$  content, which is the characteristic of more distortions of  $\text{TeO}_4$  polyhedra. The second band (shoulder) (nearly observed at  $780\text{cm}^{-1}$ ) was attributed to asymmetrical vibrations of  $\text{TeO}_4$  structural units ( $\text{O}_{\text{eq}}\text{-Te-O}_{\text{eq}}$ ). The presence of mainly  $\text{TeO}_{3+1}$  and  $\text{TeO}_3$  entities is the signature of breaking off in the tellurite matrix glass network due to a large proportion of added tantalum oxide.

The two modes observed nearly at  $780$  and  $671\text{cm}^{-1}$  can be assigned as the frequency shifts from  $\nu_1(\text{A1}) = \nu^s(\text{TeO}_4)_{\text{eq}} = 780\text{cm}^{-1}$  and  $\nu_2(\text{A1}) = 650\text{cm}^{-1}$  with the formation of  $\text{TeO}_3$  units. The downward shift of the  $\nu_s(\text{TeO}_4)_{\text{eq}}$  and  $\nu_s(\text{TeO}_4)_{\text{ax}}$  modes in the spectra of the binary  $\text{TeO}_2\text{-MO}$  (or  $\text{M}_2\text{O}$ ) systems have been reported in the literature [17-20]. According to Dimitrova- Pankova et al. [17]  $\text{TeO}_{3+1}$  structural units are formed in binary tellurite glasses containing monovalent or bivalent cations as network modifiers. For 10 mol%  $\text{TaO}_{2.5}$  we observe two bands ( $662\text{-}770\text{ cm}^{-1}$ ). With increasing modifier content, the deformation of the  $\text{TeO}_4$  polyhedra became greater, and the symmetry of the  $\text{TeO}_4$  group decreases.

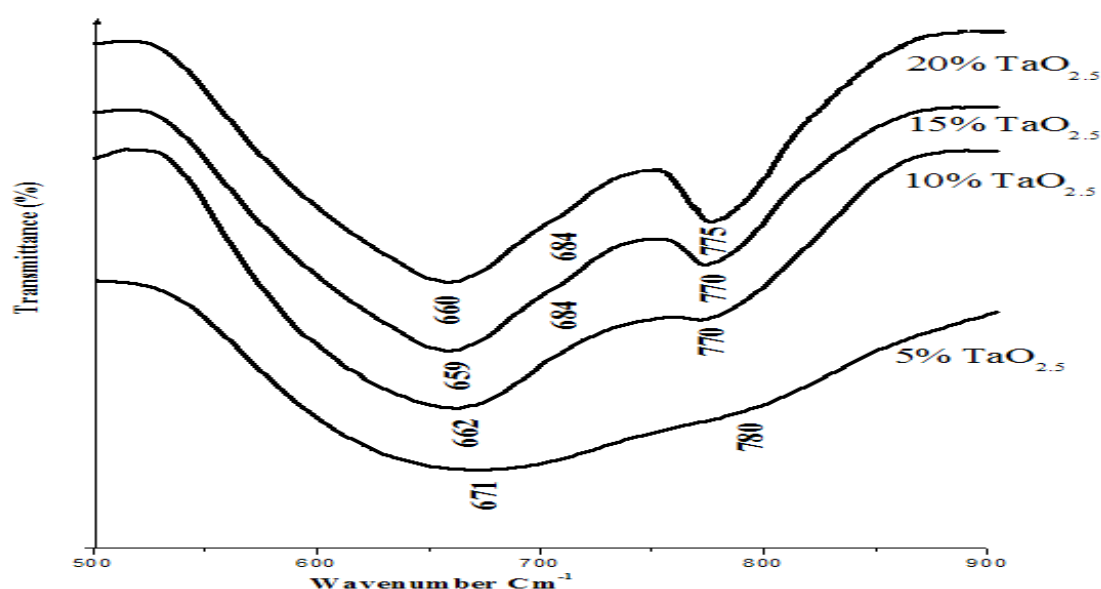


**Figure 5:** IR transmission spectra of glasses and crystalline phases of the  $\text{TeO}_2\text{-TaO}_{2.5}$  system.

### 3.3.2 Raman spectra

The Raman spectra of the pseudo binary  $\text{TeO}_2\text{-TaO}_{2.5}$  vitreous phases versus the added amount of  $\text{TaO}_{2.5}$  is illustrated in (Figure 6). For all samples, spectra obtained from different spots are identical showing high homogeneity of glasses. As shown in (Figure 6), there are two pronounced peaks occur around  $670\text{-}690\text{ cm}^{-1}$  and  $750\text{-}770\text{ cm}^{-1}$ . The most prominent band at  $680\text{ cm}^{-1}$  in the spectrum of pure glass is related to the combined vibrations of asymmetric stretching of  $\text{Te-eqOax-Te}$  bonds and symmetric stretching of  $\text{TeO}_4$  (TBP). With addition of  $\text{TaO}_{2.5}$  up to 20% mol fraction, intensity of this band decreases ( $G_1$ ), while bands at  $750\text{-}770\text{ cm}^{-1}$  ( $G_2$ ) attributed to stretching vibrations of non-bridging  $\text{Te-O-}$  bands in  $\text{TeO}_3$  (TP). The peak ( $G_2$ ), which is assigned to a stretching vibration of  $\text{TeO}_4$  units, was observed to decrease as the  $\text{TaO}_{2.5}$  contents increase. The decrease in intensity would suggest the possibility of conversion from  $\text{TeO}_4$  tbp units to the other basic structural unit [22]. The peak ( $G_1$ ) is reported to be due to the perturbation of  $\text{TeO}_4$  (TBP) units into  $\text{TeO}_3$  (trigonal pyramids) units via the intermediate coordination of  $\text{TeO}_{3+1}$  [22- 24]. Both features would clearly indicate that the network of the  $\text{TeO}_3$  structural unit increases with the increasing of  $\text{TaO}_{2.5}$  contents. Other peaks around (P)  $350\text{-}550\text{ cm}^{-1}$ , are observed to be less sensitive to the  $\text{TaO}_{2.5}$  contents. A decrease in



the peak intensity would suggest the occurrence of the destruction of Te–O–Te (or O–Te–O) in the linkages, thus resulted in the decreasing of the Te–O–Te linkages in a continue network of  $\text{TeO}_n$  ( $n = 4, 3 + 1, \text{ or } 3$ ) entities, which is consistent with the observation reported elsewhere [24], the intensity of this band decreases, while bands at  $680$  and  $760 \text{ cm}^{-1}$  were attributed to stretching vibrations of non-bridging Te–O– bands in  $\text{TeO}_3$  (TP) grow in intensity. An other peaks around  $50 \text{ cm}^{-1}$  occur in all glasses is assigned to Boson. The orthotellurate ion,  $\text{TeO}_6^{6-}$ , will have octahedral symmetry but may be strongly distorted. Vibrational modes for the tellurate anion should occur in the  $620\text{--}650 \text{ cm}^{-1}$  and in the  $290\text{--}360 \text{ cm}^{-1}$  regions [25].

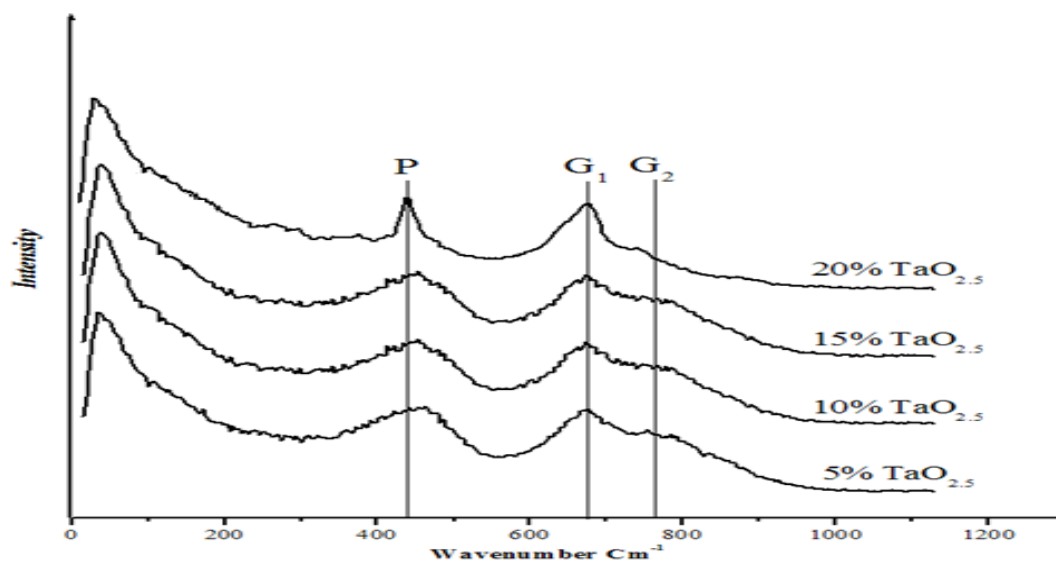


**Figure 6:** Raman spectra of glasses and crystalline phases of the  $\text{TaO}_{2.5}\text{--TeO}_2$  system.

## Conclusion

A stable glass has been synthesized in  $\text{Bi}_2\text{O}_3\text{--Ta}_2\text{O}_5\text{--TeO}_2$  system at  $850 \text{ }^\circ\text{C}$ . The vitreous crystallization of the samples rich of  $\text{TeO}_2$  occurs for the  $\alpha\text{TeO}_2$ ,  $\gamma\text{TeO}_2$  and  $\text{Ta}_2\text{Te}_3\text{O}_{11}$  polymorphs. The  $\gamma\text{TeO}_2$  variety transforms complete to  $\alpha\text{TeO}_2$  up  $550^\circ\text{C}$ .

The X ray diffraction spectra of the crystallized phases gained after a thermal annealing of the composition 85 %  $\text{TeO}_2$  15%  $\text{TaO}_{2.5}$  at a temperature of  $500 \text{ }^\circ\text{C}$  during 24h, shows the existence of a tri-phased mixture  $\text{TeO}_2$  ( $\alpha$ ),  $\text{TeO}_2$  ( $\gamma$ ) and a new phase called Y.

The densities and molar volume of the glasses decrease in  $\text{TaO}_{2.5}$  content. The characteristic temperatures (glass transition and crystallization temperatures) have been determined.

The influence of a gradual addition of the modifier oxides on the coordination geometry of tellurium atoms has been elucidated. Based on IR absorption curves and the Raman spectra of glasses show systematic changes in structural units, from  $\text{TeO}_4$  trigonal bipyramid (tbps) to  $\text{TeO}_3$  trigonal pyramid (tps) via  $[\text{TeO}_{3+1}]$  entities with increasing  $\text{TaO}_{2.5}$  content in glass.

## References

1. A. Berthereau, E. Fargin, Villezusanne A., *J. Solid State Chemistry*. 126 (1996) 143-151.
2. Jiang Li, Zhang Shian, Wang Yufei, *Chinese Opt. Lett.* 2 (2004) 53.
3. E. Yousef, M. Hotzel, C. Russel, *J. Non-Cryst. Solids* 353 (2007) 333-338.
4. A. Narazaki, K. Tanaka, Kazuyuki, *Appl. Phys. Lett.* 75 (1999) 3399.
5. Y. Wang, S. Dai, T. Xu, Nie, Q., Shen, X., Wang, X. *Acta Optica Sinica*, 28 (2008) 1751-1756

6. M.A. Villegas, J.M. Fernández Navarro, *J. Eur. Ceram. Soc.* 27 (2007) 2715.
7. L. D. Pye, H. J. Stevens and W.C. Lacourse, *Physics of Non-Crystalline Solids*, Taylor and Francis, March (1992), P. 281.
8. S. Blanchandin, P. Marchet, P. Thomas, J.-C. Champarnaud-Mesjard, B. Frit, *J. Mater. Chem.* 9 (1999) 1785.
9. J.-C. Champarnaud-Mesjard, S. Blanchandin, P. Thomas, A.P. Mirgorodsky, T. Merle-Mejean, B. Frit, *J. Phys. Chem. Solids* 61 (2000) 1499–1507.
10. S. Blanchandin, P. Thomas, P. Marchet, B. Frit and A. Chagraoui, *J. Mater. Sciences*, 34 (1999) 4285-4292.
11. S. Blanchandin, P. Thomas, P. Marchet, J.C. Champarnaud-Mesjard and B. Frit, *J. Alloys and Compounds*, 34 (2002) 206-212.
12. A. Chagraoui, A. Chakib, A. Mandil, A. Tairi, Z. Ramzi, S. Benmokhtar, *Scripta Materialia*, 56 (2007) 93.
13. A. Chagraoui, Z. Ramzi, A. Tairi, A. Mandil, M. Talibouridah, K. Ajebli and Y. Abboud, *J. Material Processing Technology*, 209 (2009) 3111-3116.
14. A. Chagraoui, I. Yakine, A. Tairi, A. Moussaoui, M. Talbi, M. Naji, *J. Mater Sci* 46 (2011) 5439–5446.
15. J.W. Visser, *J. Appl. Cryst.* 24, (1969) 987-993.
16. Sidek H.A, Hamezan M. Zaidan A.W, *J of American Applied Science* 2(8) (2005), 1266-1269.
17. M. Dimitrova-Pankova, Y. Dimitriev, M. Arnaudov, V. Dimitrov, *Phys. Chem. Glasses* 30 (6) (1989) 260–263.
18. T. Sekiya, N. Mochida, A. Ohtsuka, M. Tonokawa, Nippon Seramikkusu Kyokai Gakujutsu Ronbunshi, *J. Ceram. Soc. Jpn.* 97 (12) (1989) 1435–1440.
19. O. Noguera, T. Merle-Méjean, A.P. Mirgorodsky, M.B. Smirnov, P. Thomas, J.C. Champarnaud-Mesjard, *J. Non-Cryst. Solids* 330 (2003) 50–60.
20. Y. Dimitriev, *Chim. Chronica, New Series* 23 (1994) 361–366.
21. M. Arnaudov, V. Dimitrov, Y. Dimitriev, L. Markova, *Mater. Res. Bull.* 17 (1982) 1121–1129.
22. H. Li, Y. Su, S.K. Sundaram, *J. Non-Cryst. Solids* 402 (2001) 293–295.
23. T. Sekiya, N. Mochida, J. Ohtsuka and M. Tonokawa, Nippon Seramikkusu, Kyokai Gakujutsu Ronbunshi, 97 (1989) 1435-1440.
24. V. Nazabal, S. Todoroki, A. Nukui, T. Matsumoto, S. Suehara, T. Hondo, T. Araki, S. Inoue, C. Rivero, and T. Cardinal, *J. Non-Cryst. Solids*. 325 (2003) 1-3, 85-102
25. Ray L. Frost, Eloise C. Keeffe, *J. Raman Spectrosc.* 40 (2009) 249-252.

(2012) [www.jmaterenvirosnci.com](http://www.jmaterenvirosnci.com)